Optics Communications 347 (2015) 141–146

Contents lists available at ScienceDirect

Optics Communications

journal homepage: www.elsevier.com/locate/optcom

Point light source imaging by a three-dimensional long-imaging-depth lens

Li-Feng Zhang [a,b,c], Jia-Sheng Ye [a,b,c,d,*], Wen-Feng Sun [a,b,c,d], Sheng-Fei Feng [a,b,c,d], Xin-Ke Wang [a,b,c,d], Yan Zhang [a,b,c,d]

[a] *Department of Physics, Capital Normal University, Beijing 100048, PR China*
[b] *Beijing Key Lab of Metamaterials and Devices, Beijing 100048, PR China*
[c] *Key Lab of THz Optoelectronics, Ministry of Education, Beijing 100048, PR China*
[d] *Beijing Center for Mathematics and Information Interdisciplinary Sciences, Beijing 100048, PR China*

ARTICLE INFO

Article history:
Received 5 December 2014
Received in revised form
19 February 2015
Accepted 22 February 2015
Available online 24 February 2015

Keywords:
Long-imaging-depth lens
The Fresnel diffraction integral method
Imaging spot size
Imaging efficiency
Wavelength tolerance
Roughness tolerance

ABSTRACT

Based on Fermat's principle, we have designed a three-dimensional long-imaging-depth (LID) lens for point light source imaging. The thickness function of the designed LID lens is given analytically. Imaging properties of the designed LID lens are simulated by the Fresnel diffraction integral method. Numerical simulations demonstrate that the designed LID lens has gained a much longer imaging depth in the axial direction, in comparison with the conventional lens. In addition, compared with the conventional lens, the transverse imaging spot size and the imaging efficiency of the designed LID lens have exhibited weaker reliance on the longitudinal position within the LID region. Finally, the wavelength tolerance and roughness tolerance properties of the designed LID lens are disclosed.

1. Introduction

The lens, as one of the most commonly used optical elements, has two basic functions of focusing and imaging. In optical focusing, rather than a definite focal point of a conventional lens, the long-focal-depth (LFD) lens has a long depth of focus in the axial direction. Therefore, it has practical applications in many optical systems, such as precise alignment, optical fiber coupling, and optical interconnections. Some scientists have designed and analyzed the three-dimensional large-sized axilenses or axicons with LFD function by the scalar diffraction methods [1–5]. Other researchers have investigated the LFD cylindrical microlenses or microlens arrays based on rigorous electromagnetic theory [6–13]. All of the previous investigations are involved with the LFD properties of lenses.

On the other aspect, the long-imaging-depth (LID) property is also very important in photography, microscopy [14,15], optical information processing [16,17], and optical coherence tomography [18,19]. For instance, in photography a long imaging depth is generally expected so that we can take a clear photo of all the objects in front of the camera, including the people and the natural scenery. However, the research on the LID property of lenses is still limited. In this paper, we extend to investigate the LID properties of a three-dimensional lens. Firstly, for point light source imaging, the boundary profile of the LID lens is designed analytically. Then, imaging performances of the designed LID lens are analyzed by the scalar Fresnel diffraction integral method, which includes the actual imaging depth, the improvement ratio in the depth of image, the imaging spot size and the imaging efficiency. Thirdly, in order to extend the applications of the designed LID lens to optical communication systems or color imaging systems, its wavelength tolerance property is characterized. Finally, the roughness tolerance of the surface profile for the LID lens is researched, to disclose the accuracy requirement in practical fabrications.

This paper is organized as follows. In Section 2, the LID lens is designed, and the Fresnel diffraction integral formula for calculating the imaging field is described. Section 3 presents the imaging properties of the designed LID lens in detail, which is divided into four subsections. For quantitative characterization, several performance quantities are defined, such as the actual imaging depth, the improvement ratio in the depth of image, the imaging spot size and the imaging efficiency. In subsection 3.1, the axial LID property is explored. In subsection 3.2, the transverse imaging properties are simulated, including the transverse imaging

* Corresponding author at: Department of Physics, Capital Normal University, Beijing 100048, PR China. Fax: +86 10 68903069.
E-mail address: jsye@mail.cnu.edu.cn (J.-S. Ye).

http://dx.doi.org/10.1016/j.optcom.2015.02.042
0030-4018/

intensity distributions, the imaging spot size and the imaging efficiency. In subsection 3.3, through changing the incident wavelength, the wavelength tolerance property of the designed LID lens is researched. In subsection 3.4, the influence of surface roughness on performance of the LID lens is investigated. A brief summary is given in Section 4.

2. Formulas for the long-imaging-depth (LID) lens boundary and the Fresnel diffraction integral method

Fig. 1 depicts a schematic of a three-dimensional LID lens for point light source imaging. The *xy* plane is the incident plane, and the *z*-axis represents the propagation direction. The whole space is air, except for the LID lens. The aperture radius of the LID lens is *R*. The on-axis point light source S situates on the left side of the LID lens, whose coordinates are denoted as $(0, 0, -L)$. Here $L = l_0$ is the object distance, as shown in Fig. 1. Different from a conventional lens, the imaging distance of the LID lens is no longer a constant, but an axial range with preset imaging depth δl, as shown in Fig. 1. The imaging distance of the LID lens is given by

$$L'(\rho_1) = l_0' - \delta l/2 + \delta l(\rho_1/R)^2, \tag{1}$$

where $\rho_1 = \sqrt{x_1^2 + y_1^2}$ represents the radial distance for an arbitrary point A $(x_1, y_1, 0)$ on the front surface of the LID lens, as shown in Fig. 1; l_0' is the central imaging distance. Since ρ_1 ranges from 0 to *R*, the imaging distance is supposed to be within $[l_0' - \delta l/2, l_0' + \delta l/2]$. If the phase function of the LID lens is $\phi(\rho_1, \lambda)$, from Fermat's principle we will have

$$\frac{2\pi}{\lambda}[L + L'(\rho_1)] = \frac{2\pi}{\lambda}\sqrt{L^2 + \rho_1^2} + \phi(\rho_1, \lambda) + \frac{2\pi}{\lambda}\sqrt{\rho_1^2 + L'^2(\rho_1)}, \tag{2}$$

where λ represents the incident wavelength in air. After mathematical simplification, the phase function $\phi(\rho_1, \lambda)$ can be written explicitly as

$$\phi(\rho_1, \lambda) = \frac{2\pi}{\lambda}[L + L'(\rho_1) - \sqrt{L^2 + \rho_1^2} - \sqrt{L'^2(\rho_1) + \rho_1^2}]. \tag{3}$$

If the refractive index of the LID lens is $n(\lambda)$, the thickness of the LID lens $h(\rho_1, \lambda)$ should satisfy $2\pi[n(\lambda) - 1]/\lambda \times h(\rho_1, \lambda) = \phi(\rho_1, \lambda)$. Now, Eq. (3) can be transformed into the following form:

$$h(\rho_1, \lambda) = \frac{L - \sqrt{L^2 + \rho_1^2}}{n(\lambda) - 1} + \frac{L'(\rho_1) - \sqrt{L'^2(\rho_1) + \rho_1^2}}{n(\lambda) - 1}. \tag{4}$$

Apparently, the lens thickness in Eq. (4) is negative, which is unreal in practical applications. For this reason, a constant thickness is added so that the corrected lens thickness becomes

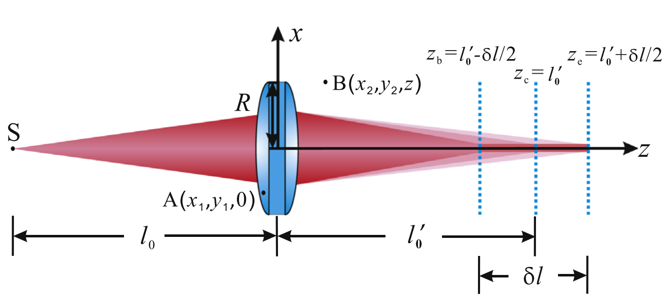

Fig. 1. A schematic for point light source imaging by a three-dimensional long-imaging-depth (LID) lens.

$$h_c(\rho_1, \lambda) = \frac{\sqrt{L^2 + R^2} - \sqrt{L^2 + \rho_1^2}}{n(\lambda) - 1} + \frac{L'(\rho_1) - L'(R)}{n(\lambda) - 1} + \frac{\sqrt{L'^2(R) + R^2} - \sqrt{L'^2(\rho_1) + \rho_1^2}}{n(\lambda) - 1}. \tag{5}$$

From Eq. (5), we know that the profile of the LID lens depends on the wavelength, the object distance, the central imaging distance, and the preset imaging depth. In this paper, parameters for designing the LID lens are chosen as follows: The designing wavelength is λ_0; the designing object distance is l_0; the designing central imaging distance is l_0'; the preset imaging depth is δl. For an arbitrary incident wavelength (λ_i, i=1,2,3,…) other than the designing wavelength (λ_0), the phase modulation of the designed LID lens is given by

$$\psi(\rho_1, \lambda_i) = \frac{2\pi[n(\lambda_i) - 1.0]}{\lambda_i} \times h_c(\rho_1, \lambda_0), \quad i = 1, 2, 3, \ldots \tag{6}$$

The point light source excites a diverging spherical wave, and the generated incident field in space is [20]

$$U_1(x, y, z, \lambda_i) = E_0 \exp(jk_i r_0)/r_0, \quad i = 1, 2, 3, \ldots \tag{7}$$

where E_0=1 is the incident amplitude; j is the imaginary unit; $k_i = 2\pi/\lambda_i$ is the wave number in air; $r_0 = \sqrt{x^2 + y^2 + (z + L)^2}$ represents the distance between the point light source S at $(0, 0, -L)$ and an arbitrary point at (x, y, z). In our simulations, both the object distance L and the imaging distance L' are in the same order of magnitude of one meter, from Eq. (5) we know that the LID lens thickness is about 100 μm. Compared with the imaging distance, the LID lens is very thin. Under thin element approximation, the scalar diffraction theory can be applied. The input field at any point A $(x_1, y_1, z = 0)$ on the front surface of the LID lens is

$$U_1(\rho_1, z = 0, \lambda_i) = \exp(jk_i\sqrt{L^2 + \rho_1^2})/\sqrt{L^2 + \rho_1^2}, \quad i = 1, 2, 3, \ldots \tag{8}$$

After passing through the lens, the phase modulation of the LID lens $\psi(\rho_1, \lambda_i)$ needs to be imposed. In our design, the lens diameter is thousands of times larger than the incident wavelength, therefore, the diffraction effect of the incident light at the edge of the LID lens can be neglected. In addition, the relation among the lens diameter, the imaging distance and the incident wavelength satisfies the Fresnel diffraction condition. Consequently, for an arbitrary observation point B (x_2, y_2, z) in the imaging space, as shown in Fig. 1, the imaging field can be computed by the Fresnel diffraction integral method as [21]

$$U_2(\rho_2, z, \lambda_i) = \int_0^R U_1(\rho_1, 0, \lambda_i) \exp\left[j\psi(\rho_1, \lambda_i) + jk_i\frac{2z^2 + \rho_1^2 + \rho_2^2}{2z}\right] J_0\left(k_i\frac{\rho_1\rho_2}{z}\right)\rho_1 \, d\rho_1, \tag{9}$$

where $\rho_2 = \sqrt{x_2^2 + y_2^2}$; J_0 is the zeroth order Bessel function. Generally, Eq. (9) should be implemented numerically. The imaging intensity distribution is obtained as $I_2 = |U_2|^2$, where $|\cdots|$ represents the magnitude of a complex number. Specially, if we assign $x_2 = y_2 = 0$, we will obtain the axial imaging intensity distribution.

3. Imaging properties of the designed LID lens

In this section, we will present the imaging properties of the designed LID lens in detail, which include the axial imaging property, the transverse imaging property, the wavelength